Improved evolution equations for magnetic island chains in toroidal pinch plasmas subject to externally applied resonant magnetic perturbations

Richard Fitzpatrick, Enrico Rossi, and Edmund P. Yu
Institute for Fusion Studies, Department of Physics, University of Texas at Austin, Austin, Texas 78712

An improved set of island evolution equations is derived that incorporates the latest advances in MHD (magnetohydrodynamical) theory. These equations describe the resistive/viscous-MHD dynamics of a nonlinear magnetic island chain, embedded in a toroidal pinch plasma, in the presence of a programmable, externally applied, resonant magnetic perturbation. A number of interesting example calculations are performed using the new equations. In particular, an investigation is made of a recently discovered class of multiharmonic resonant magnetic perturbations that have the novel property that they can lock resonant island chains in a stabilizing phase. © *2001 American Institute of Physics.* [DOI: 10.1063/1.1404384]

I. INTRODUCTION

Recent experimental results strongly suggest that further progress in obtaining thermonuclear reactor grade plasmas in either tokamaks or reversed-field pinches (RFPs) is dependent on the development of some reliable method for controlling the amplitudes of relatively low mode-number tearing modes, resonant within the plasma.[1–5] As the name suggests, "tearing modes" tear and reconnect magnetic field lines to produce helical chains of magnetic islands inside the plasma. Such island chains degrade plasma confinement because both heat and particles are able to travel radially from one side of an island chain to the other by flowing along magnetic field lines, which is a relatively fast process, instead of having to diffuse across magnetic flux surfaces, which is a relatively slow process.[6]

Currently, one of the most promising options for controlling tearing mode amplitudes in toroidal fusion devices is active feedback by means of externally applied, resonant magnetic perturbations (RMPs). Active control has already been implemented in a handful of tokamak experiments,[7–9] with some degree of success.

The most useful approach to interpreting data from RMP experiments is to reduce the problem to a set of coupled ordinary differential equations governing the phase and amplitude evolution of the target magnetic island chain.[9,10] Over the years, a great deal of effort has been put into deriving a suitable set of island evolution equations.[11–14] Our aim in the paper is to continue this effort by making available to experimentalists an improved set of evolution equations that incorporates the latest advances in MHD theory.

Our analysis is restricted to low-β, large aspect-ratio, circular cross-section, axisymmetric, toroidal plasmas. Our starting point is the standard equations of resistive/viscous MHD. Drift and two-fluid effects are completely neglected in this paper. The novel features of our island evolution equations include the following.

(i) The absence of a tokamak-specific approach. Our island evolution equations are valid for tokamaks, RFPs, and any other type of axisymmetric toroidal fusion device.

(ii) An improved treatment of nonlinear island saturation using the exact results of Thyagaraja[15] rather than the heuristic analysis of White *et al.*[16]

(iii) A vastly improved treatment of the viscous coupling between the island chain and the plasma. As discussed in Refs. 17 and 18, it is vitally important to model this coupling accurately. The analysis presented in this paper is completely general, unlike that presented in Refs. 17 and 18, where a separable form for the perturbed plasma velocity was adopted, which had the effect of excluding transient solutions. Although the exclusion of transients was a sensible approximation for the class of problems discussed in Refs. 17 and 18, it is not appropriate in this paper, which deals with programmable RMPs, which, in principal, could vary sufficiently rapidly in time to excite strong velocity transients.

(iv) A correct treatment of ion polarization (within the context of resistive/viscous MHD). Previously, it was supposed that ion polarization had a *stabilizing* effect on magnetic island chains.[14,19,20] It has since been established that just the opposite is the case—ion polarization has a *destabilizing* effect on magnetic islands.[17,21] The form for the ion polarization term presented in this paper is more general than that presented in Ref. 17, since it allows for the possibility of a multiharmonic RMP.

(v) The allowance for multiharmonic RMPs. As demonstrated recently by Fitzpatrick and Rossi,[22] nonlinear coupling in the island region allows the overtone harmonic components (i.e., jm, jn, where $j = 2,3,4,...$) of a RMP to exert a torque on an m, n island chain. In principle, it is possible to use this effect to construct a perturbation capable of locking a resonant island chain in a *stabilizing phase*. The analysis presented in this paper is considerably more general than that presented in Ref. 22 for two reasons. First, because of the incorporation of plasma rotation and viscosity into the analysis, and, second, because the variation of the coupling strength with the phase of the island chain with respect to the external perturbation is taken into account. The latter effect

is important and was neglected in Ref. 22 for the sake of simplicity.

This paper is organized as follows. After some preliminary analysis in Sec. II, we derive our improved island evolution equations in Sec. III. We then illustrate the properties of these equations by using them to analyze the standard case of a single-harmonic RMP in Sec. IV. The more interesting case of a multiharmonic RMP is considered in Sec. V. Finally, in Sec. VI, we summarize and draw some conclusions.

II. PRELIMINARY ANALYSIS

A. Plasma equilibrium

Consider a large aspect-ratio,[23] zero-β,[24] plasma equilibrium whose unperturbed magnetic flux surfaces map out (almost) concentric circles in the poloidal plane. Such an equilibrium is well approximated as a periodic cylinder. Suppose that the minor radius of the plasma is a. Standard cylindrical polar coordinates (r, θ, z) are adopted. The system is assumed to be periodic in the z direction, with periodicity length $2\pi R_0$, where R_0 is the simulated plasma major radius. It is convenient to define a simulated toroidal angle $\phi = z/R_0$. The equilibrium magnetic field is written as $\mathbf{B} = [0, B_\theta(r), B_\phi(r)]$, where $\nabla \wedge \mathbf{B} = \sigma(r)\mathbf{B}$.

B. Perturbed magnetic field

The magnetic perturbation associated with an m, n tearing mode (i.e., a mode with m periods in the poloidal direction, and n periods in the toroidal direction) can be written as $\mathbf{b}(\mathbf{r}, t) = \mathbf{b}^{m,n}(r, t)e^{i\zeta}$, where $\zeta = m\theta - n\phi$ is a helical angle. In this paper, it is assumed that $m > 0$ and $n \neq 0$. The linearized magnetic flux function $\psi^{m,n}(r, t) \equiv -irb_r^{m,n}$ satisfies Newcomb's equation.[22,25] As is well known, Newcomb's equation is *singular* at the m/n rational surface, minor radius r_s, which satisfies $F(r_s) = 0$, where $F(r) \equiv mB_\theta(r) - n\epsilon(r)B_\phi(r)$. Here, $\epsilon = r/R_0$. This singularity is resolved by the presence of a thin nonlinear/nonideal region (i.e., a magnetic island chain) centred on the rational surface.

Let $\hat{\psi}^{m,n}(r)$ represent the normalized m, n tearing eigenfunction. In other words, $\hat{\psi}^{m,n}(r)$ is a *real*, continuous solution to Newcomb's equation, which is well behaved as $r \to 0$, satisfies $\hat{\psi}^{m,n}(r_s) = 1$, and is bounded as $r \to \infty$. This prescription uniquely specifies $\hat{\psi}^{m,n}(r)$. In general, $\hat{\psi}^{m,n}(r)$ possesses a gradient discontinuity at $r = r_s$. The real quantity,

$$E_j = \left[r \frac{d\hat{\psi}^{jm,jn}(r)}{dr} \right]_{r_{s-}}^{r_{s+}}, \tag{1}$$

can be identified as the standard *linear stability index* for the jm, jn tearing mode.[26] In this paper, it is assumed that $E_1 > 0$ and $E_j < 0$ (for $j = 2,3,4,...$). In other words, the fundamental harmonic (i.e., $j = 1$) is linearly unstable, whereas the overtone harmonics (i.e., $j = 2,3,4,...$) are linearly stable.

C. Rotating resonant magnetic perturbation

Suppose that the plasma is surrounded by a set of field coils that generate a rotating magnetic perturbation, resonant with an m, n island chain inside the plasma. In general, such a perturbation consists of an admixture of m, n and jm, jn (for $j = 2,3,4,...$) magnetic fields. In the absence of the plasma, the applied perturbation takes the form $\mathbf{b}_{\mathrm{vac}} = \mathcal{C}\nabla\psi_{\mathrm{vac}} \wedge \hat{\mathbf{n}}$, where $\mathcal{C} = (m^2 + n^2\epsilon^2)^{-1/2}$, and $\hat{\mathbf{n}} = \mathcal{C}(0, n\epsilon, m)$. In the region lying within the field coils, we can write

$$\psi_{\mathrm{vac}}(r, \zeta, t) = \sum_{j=1}^{\infty} B_j \frac{i_{jm}(jn\epsilon)}{i_{jm}(jn\epsilon_a)} e^{ij[\zeta - \int_0^t v_c(t')dt']}, \tag{2}$$

where $\epsilon_a = a/R_0$. Here, the B_j are *complex* quantities that specify the amplitudes and phases of the various harmonics that make up the perturbation, whereas v_c is the common helical phase velocity of these harmonics. The function $i_m(n\epsilon)$, as well as the associated function $k_m(n\epsilon)$, are vacuum solutions to Newcomb's equation, and are defined in Ref. 22.

D. Rutherford island width evolution equation

According to the results of Rutherford,[27,28] Thyagaraja,[15] and Fitzpatrick and Waelbroeck,[17] we can write the following island width evolution equation:

$$\frac{\Lambda_1}{2}\tau_R \frac{d(W/r_s)}{dt} = E_1 - \lambda_s^2 \Lambda_1 \left(\frac{W}{4r_s}\right) \ln\left(\frac{4r_s}{W}\right) + \left(\frac{W_c}{W}\right)^2 \cos\varphi + \frac{4l_0(\tau_H \mathcal{I}_s)^2}{(W/4r_s)K_s}. \tag{3}$$

Here, $\Lambda_1 = 1.6454$, $l_0 = 2.934 \times 10^{-2}$, W is the full radial width of the m, n island chain, φ is the helical phase difference between the chain and the m, n component of the external perturbation,

$$\lambda_s = \left[\frac{r^2 d\sigma/dr}{r\sigma - 2mn\epsilon/(m^2 + n^2\epsilon^2)} \right]_{r_s}, \tag{4}$$

and

$$K_s = \frac{(n\epsilon_s)^2}{m^2 + (n\epsilon_s)^2}, \tag{5}$$

where $\epsilon_s = r_s/R_0$. The quantity W_c, which is a convenient measure of the amplitude of the external perturbation, is defined as

$$\frac{W_c}{4r_s} = \sqrt{\frac{D_1 a |b_{\mathrm{vac}\, r}^{m,n}(a)|}{F_s'}}, \tag{6}$$

where $F_s' = (r^2 dF/dr)_{r_s}$, and

$$D_j = \frac{\hat{\psi}^{jm,jn}(a)j^2(m^2 + n^2\epsilon_s^2)}{-k_{jm}(jn\epsilon_a)i_{jm}(jn\epsilon_a)}. \tag{7}$$

The quantities,

$$\tau_H = \frac{r_s^2 \sqrt{\mu_0 \rho_s}}{F_s'}, \tag{8}$$

$$\tau_V = \frac{r_s^2 \rho_s}{\mu_s}, \tag{9}$$

$$\tau_R = \frac{\mu_0 r_s^2}{\eta_s}, \tag{10}$$

represent the hydromagnetic, viscous diffusion, and resistive diffusion time scales, respectively, evaluated in the vicinity of the rational surface. Here, ρ_s, μ_s, and η_s are the plasma mass density (perpendicular), viscosity, and (parallel) resistivity, respectively, at the rational surface. Finally, $\mathcal{I}_s = [r\partial(n\Delta\Omega)/\partial r]_{r_{s-}}^{r_{s+}}$, where $\Delta\Omega$ is the modification of the plasma toroidal angular velocity profile due to the action of the external perturbation.

In writing Eq. (3), the following assumptions have been made. First, the width of the island chain, W, is assumed to be much smaller than the radial localization scale length of the perturbed plasma velocity profile, $\Delta\Omega$, in the vicinity of the rational surface. Second, strong neoclassical flow damping[29] is assumed to prevent any significant modification of the plasma poloidal velocity profile, and, hence, to give rise to an effective enhancement of ion inertia by a factor $1/K_s$.[14]

According to Eq. (3), the width of an m, n magnetic island chain evolves on a *resistive* time scale.[27] The first term on the right-hand side represents the linear instability drive.[26] The second term controls the nonlinear saturation of the island chain.[15] The third term describes the influence of the m, n component of the external perturbation on the island width.[28] Finally, the fourth term represents the *destabilizing* effect of the ion polarization current associated with perturbed plasma flow in the vicinity of the island chain.[17]

E. Phase evolution equations

In order to access whether a RMP has a stabilizing or a destabilizing influence on its target island chain, we need a method for determining the relative helical phase, φ, of the chain.

According to the results of Fitzpatrick, Waelbroeck, Yu, and Rossi,[17,18,22] the helical phase of an island chain in the presence of a RMP is obtained from the following set of equations:

$$\frac{r\rho(r)\tau_V}{r_s^2\rho_s}\frac{\partial n\Delta\Omega}{\partial t} - \frac{\partial}{\partial r}\left(r\frac{\mu}{\mu_s}\frac{\partial n\Delta\Omega}{\partial r}\right)$$
$$= -\frac{K_s}{2}\frac{\tau_V}{\tau_H^2}\left(\frac{W_c}{4r_s}\right)^2\left(\frac{W}{4r_s}\right)^2 T(\varphi)\delta(r-r_s), \tag{11}$$

and

$$\frac{d\varphi}{dt} = v^{(0)} + n\Delta\Omega(r_s,t) - v_c. \tag{12}$$

Here, $\rho(r)$ and $\mu(r)$ are the plasma mass density and (perpendicular) viscosity profiles, respectively. Moreover, $v^{(0)}$ is the so-called "natural frequency" of the island chain (i.e., the value toward which its helical phase-velocity relaxes in the absence of an external perturbation). The torque function, $T(\varphi)$, is defined in Sec. III C. Finally, the boundary conditions imposed on Eq. (11) are

$$\frac{\partial\Delta\Omega(0,t)}{\partial t} = \Delta\Omega(a,t) = 0. \tag{13}$$

Equation (11) is simply the toroidal angular equation of motion of the plasma. The term on the right-hand side represents the electromagnetic torque exerted in the island region by the RMP. Note that the radial extent of this region is assumed to be negligible compared to the radial extent of the plasma. Equation (12) is the familiar "no slip" condition,[30] which ensures that the magnetic island chain is entrained by the plasma flow in the vicinity of the rational surface. Finally, Eq. (13) enforces the physical constraint that there is no significant modification of the edge plasma rotation due to the external torque.[30]

III. DERIVATION OF ISLAND EVOLUTION EQUATIONS

A. General solution of phase evolution equations

It is helpful, at this stage, to normalize our equations. Let $\hat{\mu} = \mu/\mu_s$, $\hat{\rho} = \rho/\rho_s$, $\hat{r} = r/r_s$, $\hat{a} = a/r_s$, $V = n\Delta\Omega/v^{(0)}$, $\hat{v}_c = v_c/v^{(0)}$, and $\hat{t} = tv^{(0)}$. Equations (11), (12), and (13) reduce to

$$\frac{\hat{r}\hat{\rho}}{\nu}\frac{\partial V}{\partial \hat{t}} - \frac{\partial}{\partial \hat{r}}\left(\hat{r}\hat{\mu}\frac{\partial V}{\partial \hat{r}}\right) = -\frac{yw^{2/3}}{J_s}T(\varphi)\delta(\hat{r}-1), \tag{14}$$

$$\frac{d\varphi}{d\hat{t}} = 1 + V(1,\hat{t}) - \hat{v}_c, \tag{15}$$

$$\frac{\partial V(0,\hat{t})}{\partial \hat{r}} = V(\hat{a},\hat{t}) = 0, \tag{16}$$

where

$$\nu = \frac{1}{v^{(0)}\tau_V}, \tag{17}$$

$$w = \left(\frac{W}{W_0}\right)^3, \tag{18}$$

$$y = \frac{W_0^2 W_c^2}{W_{\text{crit}}^4}, \tag{19}$$

$$\left(\frac{W_0}{4r_s}\right)\ln\left(\frac{4r_s}{W_0}\right) = \frac{E_1}{\lambda_s^2\Lambda_1}, \tag{20}$$

$$\frac{W_{\text{crit}}}{4r_s} = \left(\frac{v^{(0)}\tau_H^2}{\tau_V}\frac{2}{K_s J_s}\right)^{1/4}, \tag{21}$$

$$J_s = \int_1^{\hat{a}}\frac{\hat{\mu}(\hat{r})}{\hat{r}}d\hat{r}. \tag{22}$$

The parameter ν is the ratio of the natural rotation period of the island chain to the viscous diffusion time scale of the plasma. The quantities w and y are convenient measures of the island width and the amplitude of the external perturbation, respectively. Finally, the parameter W_0 is the saturated island width in the absence of an external perturbation.

Let

$$\frac{d}{d\hat{r}}\left(\hat{r}\hat{\mu}\frac{du_n}{d\hat{r}}\right)+\hat{r}\hat{\rho}\beta_n u_n=0, \tag{23}$$

$$\frac{du_n(0)}{d\hat{r}}=u_n(\hat{a})=0, \tag{24}$$

$$\int_0^{\hat{a}}\hat{r}\hat{\rho}u_n u_m d\hat{r}=\delta_{n,m}. \tag{25}$$

According to standard Sturm–Liouville theory, the $u_n(\hat{r})$ are mutually orthogonal [see Eq. (25)], and form a complete set. Note that the $u_n(\hat{r})$ and the β_n can be thought of as the velocity "eigenfunctions" and "eigenvalues" of the plasma, respectively.

As is easily demonstrated, the general solution to Eq. (14) is written as

$$V(\hat{r},\hat{t})=\sum_{n=1}^{\infty}g_n(\hat{t})\frac{u_n(\hat{r})}{u_n(1)}, \tag{26}$$

where the g_n are specified in Eq. (33).

B. Island evolution equations

It is convenient to define the following normalized quantities:

$$h=\frac{1}{3\ln(4r_s/W_0)}, \tag{27}$$

$$\eta=\frac{6}{\Lambda_1}\frac{E_1}{v^{(0)}\tau_R}\frac{r_s}{W_0}, \tag{28}$$

$$L=\frac{1}{E_1}\left(\frac{W_{\text{crit}}}{W_0}\right)^4, \tag{29}$$

$$M=\frac{2l_0}{\nu J_s}\left(\frac{W_0}{4r_s}\right)^3. \tag{30}$$

Here, η is the ratio of the natural rotation period of the island chain to the island width evolution time scale. Furthermore, L controls the strength of the external perturbation term in the island width evolution equation. Finally, M measures the relative strengths of the ion polarization current and external perturbation terms in the island width evolution equation.

Our full set of normalized island evolution equations can now be written as

$$\frac{1}{\eta}\frac{dw}{d\hat{t}}=w^{2/3}[1-w^{1/3}(1-h\ln w)]+Ly\cos\varphi$$

$$+LMw^{5/3}y^2[T(\varphi)]^2, \tag{31}$$

$$\frac{d\varphi}{d\hat{t}}=1+\sum_{n=1}^{\infty}g_n-\hat{v}_c, \tag{32}$$

$$\frac{1}{\nu}\frac{dg_n}{d\hat{t}}=-yw^{2/3}\frac{[u_n(1)]^2}{J_s}T(\varphi)-\beta_n g_n. \tag{33}$$

The $u_n(\hat{r})$ and β_n are defined in Eqs. (23)–(25). The torque function $T(\varphi)$ is defined in Eq. (34). The parameters η, ν, h, L, M, and J_s are defined in Eqs. (28), (17), (27), (29), (30), and (22), respectively. Finally, the normalized amplitude, $y(\hat{t})$, and phase velocity, $\hat{v}_c(\hat{t})$ [defined in Eqs. (19) and (2), respectively] of the external perturbation are assumed to be given.

Equation (31) is our island width evolution equation. The normalized island width w is defined in Eq. (18). The first term on the right-hand side specifies the linear instability drive and the nonlinear saturation mechanism. The second term represents the influence of the external perturbation on island growth. The final term specifies the destabilizing effect of the ion polarization current.

Equations (32) and (33) are our phase evolution equations. Here, φ is the helical phase of the island chain measured with respect to the m, n component of the external perturbation, whereas the g_n parametrize the perturbed plasma velocity profile. The first equation describes how the island chain is entrained in the plasma flow at the rational surface. The second equation describes how the plasma flow is modified by the electromagnetic torque exerted in the vicinity of the rational surface by the external perturbation.

C. The torque function

The torque function, $T(\varphi)$, takes the general form

$$T(\varphi)=\sum_{j=1}^{\infty}t_j\sin(j\varphi). \tag{34}$$

In vacuum, the normalized radial component of the externally applied RMP is written as

$$\hat{r}\hat{b}_{r\text{vac}}(\hat{r},\zeta)=\sum_{j=1}^{\infty}b_j\frac{E_j}{E_1}\frac{D_1}{D_j}\frac{\Lambda_1}{\Lambda_l}\frac{i_{jm}(jn\epsilon)}{i_{jm}(jn\epsilon_a)}\sin(j\zeta), \tag{35}$$

in a corotating frame of reference. The E_j are defined in Eq. (1). The D_j are defined in Eq. (7). The $i_m(\ )$ are defined in Ref. 22. Finally, the constants Λ_j take the following values:[22] $\Lambda_1=1.6454$, $\Lambda_2=1.7058\times10^{-1}$, $\Lambda_3=-3.3174\times10^{-2}$, $\Lambda_4=1.2816\times10^{-2}$, $\Lambda_5=-6.4520\times10^{-3}$, $\Lambda_6=3.7622\times10^{-3}$, $\Lambda_7=-2.4113\times10^{-3}$, $\Lambda_8=1.6539\times10^{-3}$, etc. Here, we are assuming that all Fourier components of the perturbation are either in phase or in antiphase with one another, for the sake of simplicity. Hence, the b_j are *real* parameters. The normalizations adopted in this paper imply that $b_1=1$.

The t_j and the b_j are related as follows:

$$t_1=b_1+\kappa b_2, \tag{36}$$

$$t_2=b_2+\kappa b_3, \tag{37}$$

$$t_{j>2}=\kappa b_{j-1}+b_j+\kappa b_{j+1}, \tag{38}$$

where $\kappa=Ly/(2w^{2/3})$.

The above expressions specify how a multiharmonic RMP exerts a torque on an m, n magnetic island chain. Overtone harmonic components of the perturbation (i.e., jm, jn components, where $j=2,3,4,...$) are able to exert a torque on the chain via *nonlinear coupling* in the island region.[22] The

strength of the coupling varies with the phase of the island chain with respect to the external perturbation: this accounts for the nondiagonal transformation matrix between the t_j and the b_j. (Note that this variation was neglected in Ref. 22, for the sake of simplicity. This neglect is equivalent to the approximation $\tilde{E}_1 \rightarrow E_1$ made in Sec. V C of Ref. 22.)

Incidentally, it is helpful to define the "locking potential:" [22]

$$\mathcal{V}_{\text{lock}}(\varphi) = \int_{\varphi_0}^{\varphi} T(\varphi') d\varphi' = -\sum_{j=1}^{\infty} \frac{t_j}{j} \cos(j\varphi). \tag{39}$$

IV. SINGLE-HARMONIC RESONANT MAGNETIC PERTURBATIONS

A. Introduction

In this section, we shall concentrate on single-harmonic RMPs (i.e., perturbations with no overtone harmonic components). For this class of perturbation, our island evolution equations, (31)–(33), reduce to

$$\frac{1}{\eta} \frac{dw}{d\hat{t}} = w^{2/3}[1 - w^{1/3}(1 - h \ln w)] + Ly \cos \varphi$$

$$+ LM w^{5/3} y^2 \sin^2 \varphi, \tag{40}$$

$$\frac{d\varphi}{d\hat{t}} = 1 + \sum_{n=1}^{\infty} g_n - \hat{v}_c, \tag{41}$$

$$\frac{1}{\nu} \frac{dg_n}{d\hat{t}} = -yw^{2/3} \frac{[u_n(1)]^2}{J_s} \sin \varphi - \beta_n g_n. \tag{42}$$

In the following, we shall illustrate the typical behavior of solutions to the above equations in experimentally relevant parameter regimes.

B. Example plasma

Our example plasma is a tokamak equilibrium whose normalized current profile takes the form $\sigma(r) = \sigma(0)(1 - r^2/a^2)^{q_a/q_0 - 1}$. Here, $q_0 = 1.1$ and $q_a = 3.2$ are the central and edge values of the "safety factor," respectively.[31] We shall study the dynamics of an $m=2/n=1$ magnetic island chain, embedded in this equilibrium. The minor radius of the 2/1 rational surface is $r_s = 0.7564a$. The saturation parameter λ_s [see Eq. (4)] takes the value -5.1050. The 2/1 tearing mode is linearly unstable with stability index $E_1 = 6.765$ [see Eq. (1)]. All other tearing modes are linearly stable. The unperturbed saturated radial width of the 2/1 island chain is $W_0 = 0.164a$ [see Eq. (20)]. The parameter h [see Eq. (27)] takes the value 0.1144.

Let us adopt the physically plausible plasma density and velocity profiles $\rho(r) = \rho(0)(1 - r^2/a^2)^{1/2}$ and $\mu(r) = \mu(0) \times (1 + r^2/a^2)^3$, respectively. In the following, the perturbed velocity profile is represented as a superposition of the first 50 velocity eigenfunctions [see Eq. (26)]: i.e., we allow n to range from 1 to 50 in Eqs. (41) and (42). Convergence studies reveal that with this many eigenfunctions we can accu-

rately represent any plausible perturbed plasma velocity profile. The parameter J_s [see Eq. (22)] takes the value 0.1861.

C. Static perturbations

Consider, first of all, *static* RMPs: i.e., perturbations whose phase velocity, $\hat{v}_c$, is zero. Let us adopt the following normalized plasma parameters: $\eta = 0.1$, $\nu = 0.01$, and $L = 1$ (i.e., a Rutherford evolution time scale that is about 10 times the natural rotation period, τ, of the 2/1 island chain, and a global viscous relaxation time scale, which is about 100 τ). These parameter values are characteristic of small tokamaks such as HBT-EP (High Beta Tokamak—Extended Pulse).[9] For the moment, we shall neglect the destabilizing effect of the ion polarization current, by setting $M = 0$.

Suppose that we subject the example plasma described in Sec. IV B to the 2/1 static RMP whose waveform, $y(t)$, is shown in Fig. 1. Here, y is the normalized perturbation amplitude [see Eq. (19)]. Incidentally, we would expect $\tau \sim 0.1$ ms, in unnormalized units, for an HBT-EP-like tokamak. As can be seen, the amplitude of the external perturbation is slowly ramped up, held steady for a while, and then slowly ramped down.

Figure 2 shows the phase-velocity response of the saturated 2/1 island chain inside the plasma [obtained by solving Eqs. (40)–(42)] to the applied 2/1 static RMP pictured in Fig. 1. It can be seen that when the perturbation amplitude is relatively low, the island chain periodically speeds up and slows down as it rotates past the perturbation, but the average island phase velocity is reduced below its unperturbed value: i.e., the island chain experiences a net braking effect. However, when the perturbation amplitude exceeds a threshold value, the island chain suddenly *locks* to the external perturbation: i.e., its phase velocity is suddenly reduced to zero. Locking occurs at time (a) in Figs. 1 and 2. The island chain remains locked until the perturbation amplitude falls below a second threshold value, at which point the chain *unlocks*: i.e., it rapidly accelerates. Unlocking occurs at time (b) in Figs. 1 and 2.
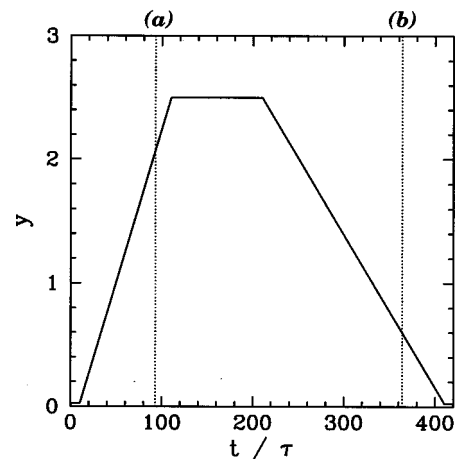

FIG. 1. Normalized amplitude of the applied 2/1 static resonant magnetic perturbation versus time. Here, τ is the rotation period of the unperturbed island chain.
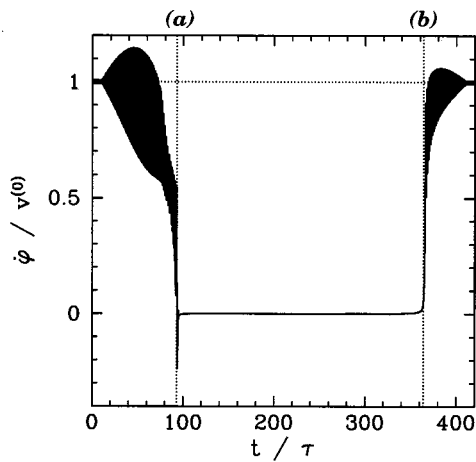
FIG. 2. Normalized 2/1 island phase velocity, versus time, for a plasma subject to the 2/1 static resonant magnetic perturbation pictured in Fig. 1. The unperturbed normalized island phase velocity is unity. The normalized plasma parameters are $\eta=0.1$, $\nu=0.01$, $L=1$, and $M=0$.

FIG. 4. Normalized width of the 2/1 magnetic island chain, versus time, for a plasma subject to the 2/1 static resonant magnetic perturbation pictured in Fig. 1. Here, W_0 is the unperturbed island width. The normalized plasma parameters are $\eta=0.1$, $\nu=0.01$, $L=1$, and $M=0$.

It is apparent, from Fig. 1, that the threshold perturbation amplitude needed to trigger locking is significantly larger than that required to trigger unlocking. This implies that once the locking threshold is exceeded, and the island chain locks to the external perturbation, the amplitude of the perturbation must be reduced by a substantial factor before the chain will unlock. This hysteresis in the locking/unlocking cycle has been observed experimentally.[32] The origin of the hysteresis is illustrated in Fig. 3.

Figure 3 shows perturbed plasma velocity profiles calculated [from Eq. (26)] just before locking [i.e., at time (a) in Fig. 2] and just before unlocking [i.e., at time (b) in Fig. 2]. Now, locking occurs when the electromagnetic torque exerted on the island chain by the external perturbation overwhelms the viscous restoring force exerted by the plasma.[30] Of course, the electromagnetic torque is proportional to the scaled amplitude, y, of the external perturbation. The viscous torque, on the other hand, is proportional to the jump in the derivative of the perturbed plasma velocity profile across the island region.[30] It can be seen, from Fig. 3, that this jump is

far larger prior to locking than prior to unlocking. The reason for this is that, prior to locking, the plasma is subject to an *oscillating* electromagnetic torque (since the island chain is rotating) that drives an *unrelaxed* perturbed velocity profile. On the other hand, prior to unlocking, the plasma is subject to a *steady* electromagnetic torque (since the island chain is static), which drives a *relaxed* velocity profile. It follows that a rotating island chain is subject to a stronger viscous restoring torque than a locked island chain. Hence, a larger electromagnetic torque (i.e., a larger perturbation amplitude) is required to lock a rotating island chain than is needed to prevent a locked chain from unlocking (once the plasma velocity profile has relaxed).

The previous discussion illustrates the importance of accurately modeling the viscous coupling between the island chain and the plasma.[17,18] In other words, it is necessary to allow the perturbed plasma velocity profile to evolve viscously in response to the applied electromagnetic torque. Most previously published sets of island evolution equations[10,14] were derived under the simplifying assumption that a fixed-width region of the plasma corotates with the island chain. Such equations are of limited use in interpreting experimental data, since they are incapable of accurately modeling the hysteresis in the locking/unlocking cycle.

Figure 4 shows the normalized width of the 2/1 island chain, versus time [obtained by solving Eqs. (40)–(42)], in the presence of the 2/1 static RMP pictured in Fig. 1. It is clear that, as long as the island chain remains unlocked, its width oscillates as it rotates past the external perturbation. Note, however, that, on average, the width of the island is *reduced* during the unlocked interval [i.e., prior to time (a), and after time (b)]. This "dynamical stabilization" effect has been observed both experimentally[9,32] and in computer simulations.[33] Unfortunately, this effect is often misinterpreted as a manifestation of the supposed *stabilizing* influence of the ion polarization current associated with strongly sheared perturbed plasma flow in the island region.[9,33] However, as has now been established beyond doubt, the ion polarization effect is, in fact, *destabilizing* (within the con-
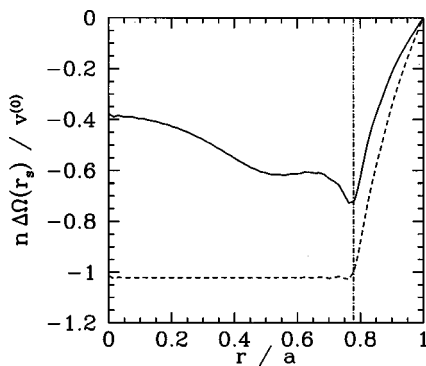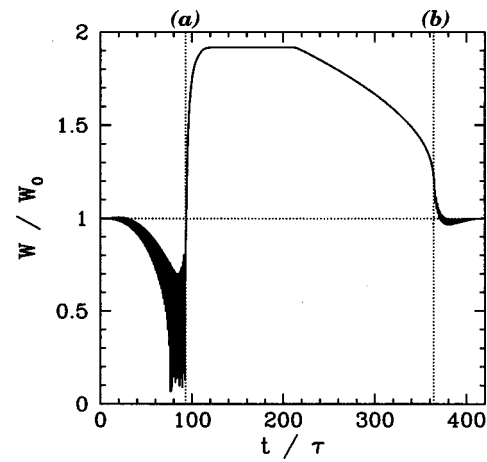

FIG. 3. Normalized perturbed plasma toroidal angular velocity profiles just before locking (solid curve) and just before unlocking (dashed curve), for a plasma subject to the 2/1 static resonant magnetic perturbation pictured in Fig. 1. The vertical line indicates the location of the 2/1 rational surface. Here, $v^{(0)}$ is the "natural frequency" of the 2/1 island chain. The normalized plasma parameters are $\eta=0.1$, $\nu=0.01$, $L=1$, and $M=0$.
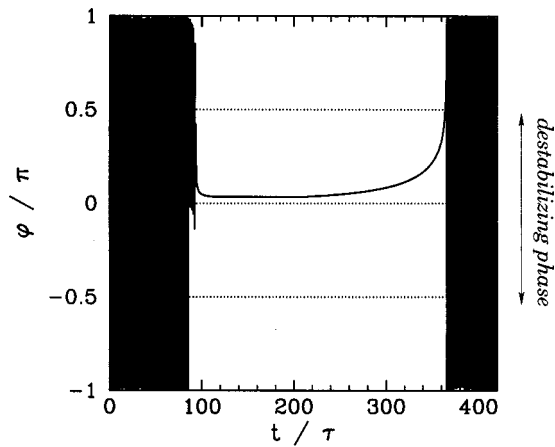
FIG. 5. Helical phase of the 2/1 magnetic island chain, versus time, for a plasma subject to the 2/1 static resonant magnetic perturbation pictured in Fig. 1. The normalized plasma parameters are $\eta = 0.1$, $\nu = 0.01$, $L = 1$, and $M = 0$.

FIG. 6. Helical phase velocity of the applied 2/1 rotating magnetic perturbation versus time. Here, $v^{(0)}$ is the "natural frequency" of the 2/1 island chain.

text of resistive/viscous MHD.[17,21] Indeed, ion polarization plays no role in the dynamics shown in Fig. 4, since we have set $M = 0$ in our island evolution equations. The explanation for the dynamic stabilization seen in Fig. 4 is quite simple.[30] As the island chain rotates past the external perturbation, it experiences an oscillating electromagnetic torque. This torque causes the island rotation to become *nonuniform*: i.e., the island chain continually speeds up and slows down as it rotates. Moreover, the nonuniformly rotating chain spends more time in the stabilizing phase [i.e., $\cos \varphi < 0$—see Eq. (40)] of the external perturbation than in the destabilizing phase (i.e., $\cos \varphi > 0$). Hence, the island chain experiences a net stabilizing effect. As is apparent from Fig. 4, this stabilization effect can become quite strong when the amplitude of the external perturbation approaches the locking threshold. Another important consequence of nonuniform island rotation is that the island chain spends more time in the helical phase in which it is *slowed down* by the electromagnetic torque [i.e., $\sin \varphi < 0$—see Eq. (42)] than the phase in which the torque causes it to *speed up* (i.e., $\sin \varphi > 0$). This accounts for the net braking effect seen in Fig. 2 prior to locking.

According to Fig. 4, as soon as the island chain *locks* to the external perturbation it is *strongly destabilized*: i.e., its width increases substantially. Figure 5 shows the helical phase of the island chain versus time. Note that during locking [i.e., between times (a) and (b) in Fig. 4] the island chain always maintains a *destabilizing* phase relation with respect to the external perturbation (i.e., $-\pi/2 < \varphi < \pi/2$). This is a standard result in MHD theory.[30] It can be seen, from Fig. 5, that as the amplitude of the external perturbation is ramped down, and the electromagnetic locking torque consequently decreases, the viscous restoring torque rotates the locked island phase toward the stabilizing region (i.e., towards $\varphi > \pi/2$), but that the island chain unlocks before stabilization is achieved. Indeed, conventional wisdom holds that a magnetic island chain can *never* lock in a stabilizing phase relation to a RMP. It follows that magnetic feedback stabilization of tearing modes is only feasible if locking is prevented—
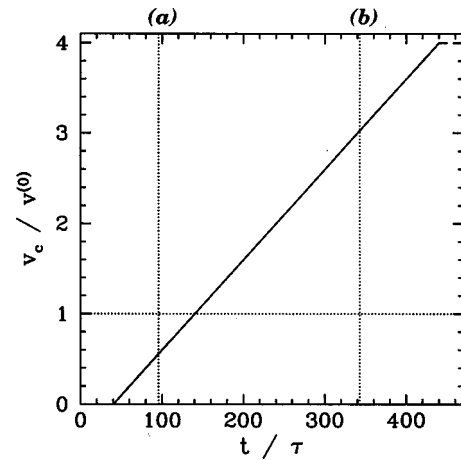
this is usually achieved by modulating the phase of the external perturbation on a faster time scale than that required for locking.[11] Unfortunately, such rapid phase modulation of a RMP would almost certainly require generating field coils located *within* the vacuum vessel (otherwise, the perturbation would be shielded from the plasma by eddy currents), which is not reactor relevant.

As can be seen from Fig. 4, the island width is generally reduced below its unperturbed value in the unlocked interval, whereas it is enhanced in the locked interval. Since the electromagnetic locking torque is proportional to the product of a scaled perturbation amplitude, y, and the square of the island width, W [see Eq. (42)], this implies that a fixed amplitude external perturbation generally exerts a larger locking torque on a locked, rather than an unlocked, island chain. This effect tends to deepen the previously mentioned hysteresis in the locking/unlocking cycle, although it is not its primary cause.

D. Rotating perturbations

Let us now consider *rotating* RMPs. For this study, we shall employ the following normalized plasma parameters: $\eta = 0.1$, $\nu = 0.01$, $L = 1$, and $M = 0.1$. These parameters are the same as those used in our previous study, except that we are now explicitly taking into account the destabilizing effect of the ion polarization current, by setting $M = 0.1$. This value for M is characteristic of small tokamaks such as HBT-EP.

Suppose that we subject the example plasma described in Sec. IV B to the 2/1 rotating RMP whose normalized helical phase velocity, $\hat{v}_c(t)$, is shown in Fig. 6. As can be seen, the rotation frequency (i.e., phase velocity) of the perturbation is ramped linearly from zero to a final value that is four times the "natural frequency" of the target 2/1 island chain inside the plasma. The perturbation amplitude is rapidly ramped up at time $t = 40\tau$, held steady at the normalized value $y = 0.9$, and then rapidly ramped down at $t = 440\tau$.

Figure 7 shows the phase-velocity response of the saturated 2/1 island chain inside the plasma to the applied 2/1 rotating RMP pictured in Fig. 6. It can be seen that when the rotation frequency (i.e., phase velocity) of the perturbation
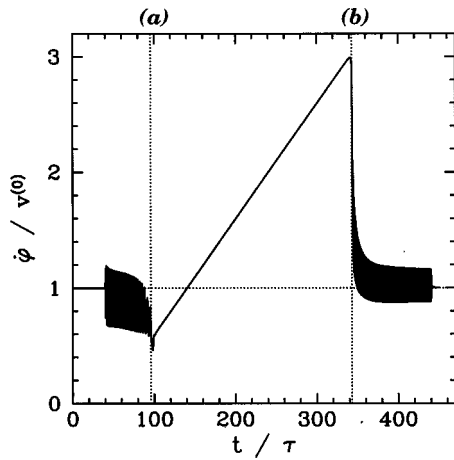
FIG. 7. Normalized 2/1 island phase velocity, versus time, for a plasma subject to the 2/1 rotating magnetic perturbation pictured in Fig. 6. Here, $v^{(0)}$ is the ''natural frequency'' of the island chain. The normalized plasma parameters are $\eta=0.1$, $\nu=0.01$, $L=1$, and $M=0.1$.
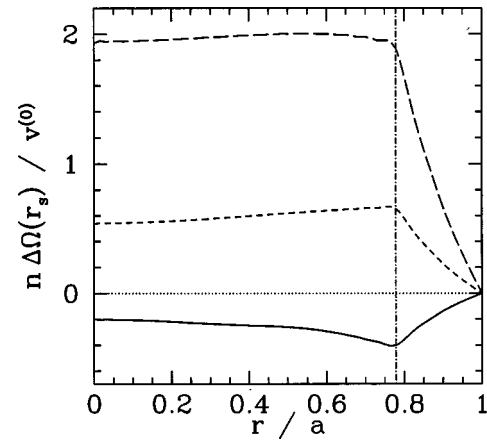

FIG. 8. Normalized perturbed plasma toroidal angular velocity profiles just before locking (solid curve), halfway between locking and unlocking (short-dashed curve), and just before unlocking (long-dashed curve), for a plasma subject to the 2/1 rotating magnetic perturbation pictured in Fig. 6. The vertical line indicates the location of the 2/1 rational surface. Here, $v^{(0)}$ is the ''natural frequency'' of the 2/1 island chain. The normalized plasma parameters are $\eta=0.1$, $\nu=0.01$, $L=1$, and $M=0.1$.

lies too far below the ''natural frequency'' of the island chain, the chain remains unlocked. In this interval, the chain's rotation frequency oscillates about an average value that is *less* than its natural value: i.e., there is a net breaking effect. However, once the (magnitude of the) difference between the perturbation frequency and the ''natural frequency'' of the island chain falls below a threshold value, the island chain suddenly *locks* to the perturbation: i.e., its rotation frequency becomes identical to that of the perturbation. Locking occurs at time (a) in Fig. 7. In the locked interval, the island chain's rotation frequency is swept upward by the perturbation, eventually reaching a value that is almost three times its natural value. However, when the difference between the perturbation frequency and the ''natural frequency'' of the island chain exceeds a second critical value, the island chain suddenly *unlocks*: i.e., it suddenly decelerates. Unlocking occurs at time (b) in Fig. 6. After unlocking, the island rotation frequency oscillates around a value that slightly *exceeds* its natural value.

It is apparent, from Fig. 7, that the threshold (magnitude of the) difference between the frequency of the external perturbation and the natural frequency of the island chain needed to trigger locking is substantially smaller than that required to trigger unlocking. This is another manifestation of the hysteresis in the locking/unlocking cycle discussed earlier. Moreover, the explanation for this hysteresis is the same as before.

Figure 8 shows perturbed plasma velocity profiles calculated just before locking [i.e., at time (a) in Fig. 7], just before unlocking [i.e., at time (b) in Fig. 7], and at some intermediate time. Clearly, a rotating RMP is very effective at injecting toroidal angular momentum into a tokamak plasma. Note that the driven velocity profile is fairly flat inside the rational surface, but strongly sheared outside. Momentum injection via rotating RMPs has been successfully demonstrated on both JFT-2M[34] and HBT-EP.[9] Jensen and Leonard[35] have suggested that this mechanism could be used to control velocity shear within tokamak plasmas. The principle objection to such a scheme is that it only works effec-

tively when the perturbation *locks* a resonant island chain inside the plasma—unfortunately, as soon as the island chain locks to the perturbation, it is *strongly destabilized* (see Fig. 9), and consequently degrades the plasma energy confinement.

Figure 9 shows the normalized width of the 2/1 island chain, versus time, in the presence of the 2/1 rotating RMP pictured in Fig. 6. As before, the island chain is strongly stabilized by the applied perturbation prior to locking [i.e., prior to time (a)]. Likewise, the chain is strongly destabilized during the locked phase [i.e., between times (a) and (b)]. However, unlike the previous case, the island chain is *destabilized* by the perturbation after unlocking [i.e., after time (b)]. This new effect is a manifestation of the destabilizing influence of the ion polarization current (which was not previously included in our calculations). It turns out that when
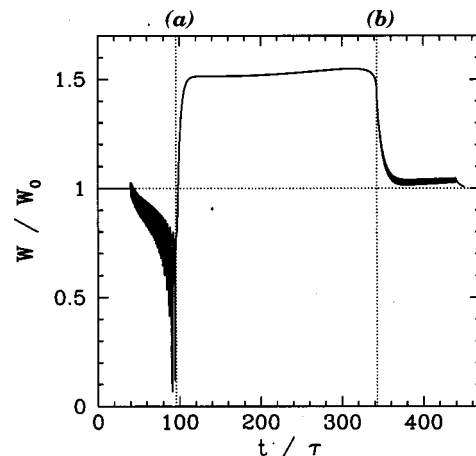

FIG. 9. Normalized width of the 2/1 magnetic island chain, versus time, for a plasma subject to the 2/1 rotating magnetic perturbation pictured in Fig. 6. Here, W_0 is the unperturbed island width. The normalized plasma parameters are $\eta=0.1$, $\nu=0.01$, $L=1$, and $M=0.1$.

the island chain is not locked to the external perturbation it is subject to *two* distinct ''inertial'' effects. The first effect is the previously mentioned nonuniform island rotation, which causes the chain to spend more time in the stabilizing phase of the external perturbation than the destabilizing phase. The second effect is the destabilizing influence of the ion polarization current associated with perturbed plasma flow in the island region. It turns out that the stabilizing influence of nonuniform island rotation is relatively *strong* when the (magnitude of the) frequency difference between the applied perturbation and the island is *small*, and relatively weak otherwise.[30] On the other hand, the destabilizing influence of the ion polarization current is essentially frequency independent [see Eq. (40)]. Hence, the former effect dominates the latter just prior to locking (when the frequency difference is relatively small), and *vice versa* just after unlocking (when the frequency difference is relatively large). We conclude that hysteresis in the locking/unlocking cycle, combined with the different frequency dependences of the two previously mentioned inertial effects, gives rise to a situation where an unlocked island chain is inertially *stabilized* when it is being *slowed down* by an external perturbation, and inertially *destabilized* when it is being *sped up*—at least, in frequency ramp experiments. This conclusion is of great interest, since it seems to be in accordance with recent experimental results from HBT-EP.[36]

V. MULTIHARMONIC RESONANT MAGNETIC PERTURBATIONS

A. Introduction

Let us now consider *multiharmonic* RMPs (i.e., perturbations with overtone harmonic components). For the sake of simplicity, we shall restrict our investigation to *static* perturbations. For this class of perturbation, we need to employ our full set of island evolution equations, (31)–(33). In particular, we must explicitly calculate the form of the *torque function*, $T(\varphi)$ (see Sec. III C).

B. Locking potentials

Now, a torque function is most conveniently described in terms of its associated *locking potential*—see Eq. (39). Figure 10 shows the locking potential, $\mathcal{V}_{\text{lock}} = -\cos \varphi$, associated with a conventional single-harmonic RMP. In the absence of plasma rotation, we would expect a resonant magnetic island chain to lock to such a perturbation at the *minimum* of the potential. This is equivalent to saying that the chain always locks in the *most destabilizing* phase, $\varphi = 0$—see Eq. (40). Plasma rotation tends to shift the locking angle away from $\varphi = 0$ (see Fig. 5). However, as a general rule of thumb, the locking angle is restricted to the *lower half* of the potential: i.e., the region $\mathcal{V}_{\text{lock}} < 0$. This observation leads to the well-known result that a resonant island chain always locks to a single-harmonic RMP in a *destabilizing phase*: i.e., $|\varphi| < \pi/2$.

In Ref. 22, we introduced the concept of a ''designer'' RMP. This is a multiharmonic perturbation in which the amplitudes and phases of the overtone harmonic components
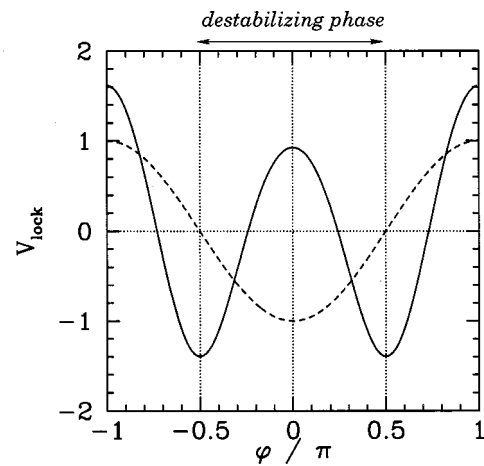

FIG. 10. Locking potentials. The dashed curve shows the locking potential $\mathcal{V}_{\text{lock}} = -\cos \varphi$ associated with a single-harmonic RMP. The solid curve shows the potential associated with a ''designer'' perturbation characterized by $b_1 = 1.0$, $b_2 = -2.92$, $b_3 = 1.0$, and $b_{j>3} = 0.0$. In the latter case, the coupling parameter κ takes the value 0.254.

are specially chosen so as to construct a locking potential capable of maintaining a resonant island chain in a *stabilizing* phase. As explained in Ref. 22, the physics basis for designer perturbations is the fact that nonlinear coupling in the island region allows *jm, jn* (where $j = 2,3,4,...$) magnetic perturbations to exert small torques on an *m, n* island chain. Figure 10 shows the locking potential associated with a three-harmonic designer perturbation characterized by $b_1 = 1.0$, $b_2 = -2.92$, $b_3 = 1.0$, and $b_{j>3} = 0.0$. In Sec. III C we explain how the vacuum, radial, magnetic perturbation that generates this potential can be calculated using the above b_j values. Incidentally, the coupling constant κ, appearing in the transformation (36)–(38), takes the value 0.254 (this value is chosen to be consistent with the following example calculation). It can be seen, from Fig. 10, that nonlinear coupling between the fundamental and overtone harmonics in the island region generates a locking potential that is *radically different* from a conventional potential. In particular, the minima of the potential now lie on the *boundary* of the destabilizing region, rather than at its *midpoint*. Adopting the usual rule of thumb that the locking angle is restricted to the lower half of the potential, it certainly seems plausible that our designer perturbation could lock a resonant island chain in a stabilizing phase (i.e., $|\varphi| > \pi/2$). Let us investigate further.

C. Designer perturbations

Let us apply the designer perturbation discussed above to the example plasma described in Sec. IV B. Of course, the fundamental harmonic of the perturbation is 2/1. Moreover, the perturbation is assumed to be static. Finally, the amplitude of the perturbation is ramped from zero to a normalized value of $y = 1$ between $t = 10\tau$ and $t = 20\tau$. The perturbation amplitude is subsequently held steady at $y = 1$. The chosen plasma parameters are $\eta = 0.1$, $\nu = 0.01$, $L = 0.35$, and $M = 0$.
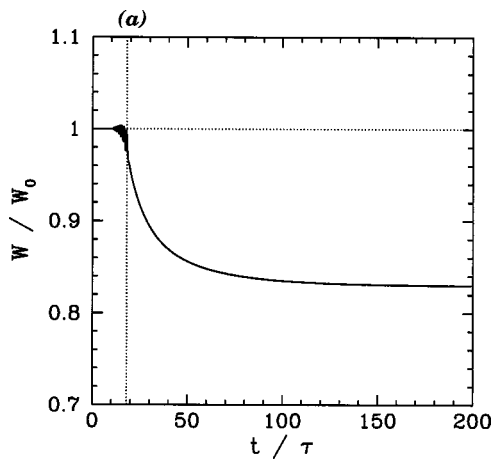
FIG. 11. The normalized width of the 2/1 magnetic island chain, versus time, for a plasma subject to the designer perturbation shown in Fig. 10. Here, W_0 is the unperturbed island width. The normalized plasma parameters are $\eta = 0.1$, $\nu = 0.01$, $L = 0.35$, and $M = 0$.

Figure 11 shows the normalized 2/1 island width, versus time, in the presence of the designer perturbation described above. The island chain locks to the perturbation at time (a). Note, however, that the island width *decreases* after locking. This behavior—which is *unprecedented* within MHD theory—suggests that the island chain does indeed lock to the perturbation in a *stabilizing phase*. This suggestion is confirmed by Fig. 12, which shows the helical phase of the island chain versus time.

Note, from Fig. 11, that the designer perturbation only reduces the island width by a modest amount (i.e., about 20%). We find that any attempt to obtain a greater reduction in island width invariably fails—either the island chain unlocks or the locking angle drifts into the destabilizing region. This behavior is easily understood. A designer perturbation only works properly provided it is able to *lock* its target island chain, and provided that the nonlinear coupling in the island region is sufficiently strong to generate a favorably shaped locking potential from the component harmonics of the perturbation. Unfortunately, the locking torque and the

strength of the nonlinear coupling in the island region both *decrease* as the island width decreases. It follows that if a designer perturbation reduces the width of its target island chain by too great a factor then it ceases to be effective.

VI. SUMMARY AND DISCUSSION

We have derived an improved set of island evolution equations that incorporate the latest advances in MHD theory—see Sec. III. These equations describe the resistive/viscous-MHD dynamics of a nonlinear magnetic island chain (embedded in a large aspect-ratio, low-β, circular cross section, toroidal pinch plasma) in the presence of a programmable, externally applied, resonant magnetic perturbation (RMP). Our equations are fairly simple in form, and, hence, can be very rapidly integrated. Indeed, none of the example calculations described in this paper took more than about 60 s of CPU (central processor unit) time on an ordinary desktop computer. In fact, it would be quite feasible to employ our equations during the *real time* analysis of data from RMP experiments.

We have performed a number of example calculations using our equations. The purpose of these calculations is to illustrate the typical behavior of solutions to our equations in experimentally relevant parameter regimes.

For the case of a static (i.e., nonrotating) single-harmonic RMP (see Sec. IV C), we find that the island chain *locks* to the perturbation when the perturbation amplitude exceeds a certain critical value, and *unlocks* when the perturbation amplitude falls below a second, much smaller, value. The main cause of this *hysteresis* in the locking/unlocking cycle is the viscous evolution of the perturbed plasma velocity profile. It turns out that the profile is generally quite different (and, hence, the viscous restoring force acting on the island chain is quite different) just prior to locking, and just prior to unlocking. This observation underscores the need to treat the viscous coupling between the island chain and the plasma in a fairly sophisticated manner. Simply assuming that a fixed-width region of the plasma corotates with the island chain invariably leads to highly inaccurate estimates of locking and unlocking thresholds.

When the island chain is not locked to the external perturbation it generally experiences a net *stabilizing* effect. This effect is often misinterpreted as a manifestation of the supposed stabilizing influence of the ion polarization current associated with perturbed plasma flow in the island region (this effect is actually destabilizing). In fact, the explanation is generally much simpler. As the island chain rotates past the perturbation, it experiences an oscillating electromagnetic torque. This torque causes the island rotation to become *nonuniform*. The nonuniformly rotating island chain spends more time in the phase in which it is stabilized by the external perturbation than in the opposite phase. Consequently, the chain experiences a net stabilizing effect. As demonstrated in our example calculations, this effect becomes particularly strong as the locking threshold is approached. On the other hand, the effect is fairly weak well away from the locking threshold.
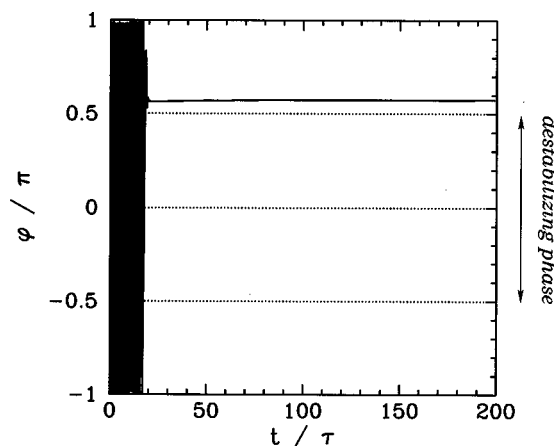

FIG. 12. Helical phase of the 2/1 magnetic island chain, versus time, for a plasma subject to the designer perturbation shown in Fig. 10. The normalized plasma parameters are $\eta = 0.1$, $\nu = 0.01$, $L = 0.35$, and $M = 0$.

Our example calculations also show that the island chain is *strongly destabilized* as soon as it locks to a single-harmonic RMP. This occurs because the chain always locks in a *destabilizing phase*. Indeed, conventional wisdom holds that a magnetic island chain must always lock to a RMP in a destabilizing phase.

For the case of a single-harmonic, constant amplitude RMP whose rotation frequency is ramped steadily upward (see Sec. IV D), we find that the island chain *locks* to the perturbation when the (magnitude of the) difference between the rotation frequency and the "natural frequency" of the island chain falls below a critical value, and *unlocks* when the same frequency difference exceeds a second, much greater, value. This is another manifestation of the hysteresis in the locking/unlocking cycle discussed above. Moreover, the basic explanation is the same. As before, the island chain is strongly destabilized when it locks to the perturbation. However, during the interval when the chain is not locked it is subject to *two* competing "inertial" effects. The first is the *stabilizing* effect of nonuniform island rotation discussed above. It turns out that the strength of this effect is a strongly decreasing function of the (magnitude of the) difference between the perturbation's rotation frequency and that of the island chain. The second effect is the *destabilizing* influence of the ion polarization current associated with perturbed plasma flow in the island region. It turns out that this effect is essentially frequency independent. Under certain circumstances, the combination of hysteresis in the locking/unlocking cycle, and the different frequency dependences of the two above-mentioned inertial effects, leads to a situation in which the island chain is *stabilized* when the perturbation rotates *more slowly* than the chain, and *destabilized* when the perturbation rotates *more quickly*. This behavior seems to be in accordance with recent experimental results from HBT-EP.[36]

For the case of a static, multiharmonic RMP (see Sec. V), we find that nonlinear coupling in the island region, combined with a judicious selection of the amplitudes and phases of the different harmonics that constitute the RMP, allow the island chain to lock to the perturbation in a *stabilizing phase*. We term a RMP capable of achieving this novel feat a "designer" perturbation, just to emphasize that a harmonic mix must be chosen *very carefully*. In our example calculations, we employ a three-harmonic designer perturbation (i.e., a particular mix of 2/1, 4/2, and 6/3 magnetic fields). Unfortunately, we find that our designer perturbation can only squeeze a locked magnetic island chain by a modest amount before the chain either unlocks, or slips into a destabilizing phase relation with respect to the perturbation. The problem is that both the locking torque—required to maintain the chain at constant phase—and the nonlinear coupling in the island region—required to permit locking in a stabilizing phase—both decrease as the island width is reduced.

Despite the limitation discussed above, designer RMPs have a number of interesting potential applications to the magnetic fusion program. The first application relates to the idea of Jensen and Leonard[35] of employing rotating RMPs to control velocity shear inside tokamaks. The eventual aim would be to enhance confinement by driving enough velocity shear to suppress plasma turbulence. As we have seen, rotating RMPs are a very effective means of injecting angular momentum into a toroidal plasma (see Sec. IV D). Moreover, the driven velocity profiles are highly sheared in the outer regions of the plasma. The usual objection to the Jensen and Leonard scheme is that RMP momentum injection only works efficiently when the perturbation *locks* a resonant island chain within the plasma. However, as soon as the island chain locks to a conventional single-harmonic RMP, it is strongly destabilized, and consequently grows, leading to a degradation in plasma confinement. Suppose, however, that we implement the Jensen–Leonard scheme with rotating, multiharmonic RMPs that are specially designed so as to lock resonant magnetic island chains in *neutral* phases: i.e., in phases such that the islands are neither stabilized nor destabilized by the perturbations. From what we have seen in our example calculations, this seems eminently feasible. In this case, it would be possible to tailor the plasma rotation profile via rotating RMPs without directly destabilizing the island chains within the plasma. Such a scheme is probably not reactor relevant (since the RMP coils would have to be placed inside the first wall to avoid eddy-current shielding); however, it could well lead to some invaluable experimental insights into the relationship between velocity shear and turbulence.

The second application of designer RMPs relates to *neoclassical tearing modes* (NTMs) in tokamaks. As is well known, a NTM is an *intrinsically stable* tearing mode that possesses a *metastable state* in which a nonlinear island chain is maintained in the plasma by the perturbed bootstrap current.[37] A NTM is ordinarily stable, but can be kicked into its metastable state by the transient magnetic perturbations generated by sawtooth crashes, ELMs (edge-localized modes), etc. However, a NTM magnetic island generally only needs to be squeezed by a moderate amount in order to trigger the reverse transition to its stable state. Suppose that we apply a static, multiharmonic RMP to a tokamak plasma subject to NTMs. Suppose, further, that the RMP is specially designed so as to lock resonant island chains in a *stabilizing* phase. When a resonant NTM is triggered, it will grow, lock to the RMP in a stabilizing phase, and (hopefully) be squeezed out of existence. As we have seen, designer perturbations can only squeeze locked island chains by a moderate amount—fortunately, this is all that is generally required to stabilize NTMs. The beauty of this scheme is that the applied RPM is *static*, so its generating coils can be placed *outside* the first wall, which is highly reactor relevant. Moreover, no detection equipment or feedback circuits are required. In contrast, magnetic feedback using conventional, single-harmonic RMPs requires fast phase modulation of the applied perturbation, in order to prevent locking—since island chains always lock to conventional RMPs in a destabilizing phase.[11] Unfortunately, such rapid phase modulation of a RMP would almost certainly require generating field coils located *within* the first wall (otherwise, the perturbation would be shielded from the plasma by eddy currents), which is not reactor relevant.

[1] T. Taylor, E. J. Strait, L. L. Lao et al., Phys. Plasmas **2**, 2390 (1995).

[2] T. Ivers, E. Eisner, A. Garafalo et al., Phys. Plasmas **3**, 1926 (1996).

[3] O. Sauter, R. J. La Haye, Z. Chang et al., Phys. Plasmas **4**, 1654 (1997).

[4] J. S. Sarff, N. E. Lanier, S. C. Prager, and M. R. Stoneking, Phys. Rev. Lett. **78**, 62 (1997).

[5] M. N. Rosenbluth, Plasma Phys. Controlled Fusion **41**, A99 (1999).

[6] Z. Chang and J. D. Callen, Nucl. Fusion **30**, 219 (1990).

[7] V. V. Arsenin, L. I. Artemenkov, N. V. Ivanov et al., in *Plasma Physics and Controlled Nuclear Fusion Research 1978*, Proceedings of the 16th International Conference, Innsbruck (International Atomic Energy Agency, Vienna, 1979), Vol. 1, p. 233.

[8] A. W. Morris, T. C. Hender, J. Hugill et al., Phys. Rev. Lett. **64**, 1254 (1990).

[9] G. A. Navratil, C. Cates, M. E. Mauel et al., Phys. Plasmas **5**, 1855 (1998).

[10] H. Zohm, A. Kallenbach, H. Bruhns, G. Fussmann, and O. Klüber, Europhys. Lett. **11**, 745 (1990).

[11] E. Lazzaro and M. F. F. Nave, Phys. Fluids **31**, 1623 (1988).

[12] G. Bosia and E. Lazzaro, Nucl. Fusion **31**, 1003 (1990).

[13] G. D'Antonia, IEEE Trans. Nucl. Sci. **41**, 216 (1994).

[14] A. I. Smolyakov, A. Hirose, E. Lazzaro, G. B. Re, and J. D. Callen, Phys. Plasmas **2**, 1581 (1995).

[15] A. Thyagaraja, Phys. Fluids **24**, 1716 (1981).

[16] R. B. White, D. A. Monticello, M. N. Rosenbluth, and B. V. Waddell, Phys. Fluids **20**, 800 (1977).

[17] R. Fitzpatrick and F. L. Waelbroeck, Phys. Plasmas **7**, 4983 (2000).

[18] R. Fitzpatrick and E. P. Yu, Phys. Plasmas **7**, 3610 (2000).

[19] M. Zabiego and X. Garbet, Phys. Plasmas **1**, 1890 (1994).

[20] H. R. Wilson, J. W. Connor, R. J. Hastie, and C. C. Hegna, Phys. Plasmas **3**, 248 (1996).

[21] F. L. Waelbroeck and R. Fitzpatrick, Phys. Rev. Lett. **78**, 1703 (1997).

[22] R. Fitzpatrick and E. Rossi, Phys. Plasmas **8**, 2760 (2001).

[23] The standard large aspect-ratio ordering is $R_0/a \gg 1$, where R_0 and a are the major and minor radii of the plasma, respectively.

[24] The conventional definition of this parameter is $\beta = 2\mu_0 \langle p \rangle / \langle B^2 \rangle$, where $\langle \cdots \rangle$ denotes a volume average, p is the plasma pressure, and B is the magnetic field strength.

[25] W. A. Newcomb, Ann. Phys. (N.Y.) **10**, 232 (1960).

[26] H. P. Furth, J. Killeen, and M. N. Rosenbluth, Phys. Fluids **6**, 459 (1963).

[27] P. H. Rutherford, Phys. Fluids **16**, 1903 (1973).

[28] P. H. Rutherford, in *Basic Physical Processes of Toroidal Fusion Plasmas*, Proceedings of the Course and Workshop, Varrena, 1985 (Commission of the European Communities, Brussels, 1986), Vol. 2, p. 531.

[29] T. H. Stix, Phys. Fluids **16**, 1260 (1973).

[30] R. Fitzpatrick, Nucl. Fusion **33**, 1049 (1993).

[31] In a large aspect-ratio, low-β, tokamak, the safety factor is defined as $q = r B_\phi / (R_0 B_\theta)$.

[32] T. C. Hender, R. Fitzpatrick, A. W. Morris et al., Nucl. Fusion **32**, 2091 (1992).

[33] G. Kurita, T. Tuda, M. Azumi, and T. Takeda, Nucl. Fusion **32**, 1899 (1992).

[34] K. Oasa, H. Aikawa, Y. Asahi et al., *Plasma Physics and Controlled Nuclear Fusion Research 1994*, Proceedings of the 15th International Conference, Seville (International Atomic Energy Agency, Vienna, 1995), Vol. 2, p. 279.

[35] T. H. Jensen and A. W. Leonard, Phys. Fluids B **3**, 3422 (1991).

[36] D. Maurer (private communication, 2000).

[37] R. Fitzpatrick, Phys. Plasmas **2**, 825 (1995).